Supporting Information

Facile Construction of Polyoxometalate-Polymer Hybrid Nanoparticles with pH/Redox Dual-Responsiveness

Yanting Gao [a][b], Fan Yang [a], Yufu Wang [a], Angus P. R. Johnston [c], Rebekah N. Duffin [b], Philip C. Andrews [b], Chris Ritchie [b] and Georgina K. Such [a]**

[a] School of Chemistry, The University of Melbourne, Parkville, 3010, Victoria, Australia

[b] School of Chemistry, Monash University, Clayton, 3800, Victoria, Australia

[c] Monash Institute of Pharmaceutical Sciences, Monash University, Parkville, Victoria 3052, Australia

*E-mail for Christopher Ritchie: chris.ritchie@monash.edu
*E-mail for Georgina Such: gsuch@unimelb.edu.au

Table of Contents

Materials

4-Cyano-4-[(dodecylsulfanylthiocarbonyl)sulfanyl]pentanoic acid (Sigma-Aldrich, 97% HPLC), 2,2'- Azobis(2-methylpropionitrile) (Sigma-Aldrich, 98%), Sodium tungstate (Combi-blocks), Boric acid (Combi-blocks), Potassium chloride (Sigma-Aldrich), Cobalt Chloride (Combi-blocks), Ammonium persulfate (Sigma-Aldrich, 98%), Tetraoctylammonium bromide (Combi-blocks), Methacrylic acid (Sigma-Aldrich), 4-Pyridinemethanol (Sigma-Aldrich), 4-Dimethylaminopyridine (Sigma-Aldrich) and all solvents were used without modification.
2-(Diethylamino)ethyl methacrylate (DEAEMA) (Sigma-Aldrich, 99%), 2-(Diisopropylamino)ethyl methacrylate (DPAEMA) (Sigma-Aldrich, 97%) and poly(ethylene glycol methacrylate) (PEGMA) (Sigma-Aldrich, average Mn 300 Da) were passed over aluminum oxide (activated, basic; Sigma-Aldrich) to remove inhibitors before use. The water used in chemistry experiments was the reverse osmosis water (RO water).

Characterization

Nuclear Magnetic Resonance (NMR)

^{1}H NMR spectroscopy was performed on a Varian 400 MHz NMR Spectrometer, carbon decoupled and referenced against residual solvent as indicated throughout.

Chemical shifts (δH) were reported in ppm. Deuterated chloroform ($CDCl_3$: δH 7.26 ppm), deuterium oxide (D_2O: δH 4.79 ppm) and deuterated acetone ($CDCl_3$: δH 2.05) were used as solvents for ^1H NMR characterization.

Dynamic light scattering (DLS)
Particle size, polydispersity and light scattering intensity determination were recorded using a Horiba Scientific SZ-100, dynamic light scattering instrument at a fixed scattering angle of 90° and a temperature of 37 °C.

Size-exclusion Chromatography (SEC)
SEC analysis was conducted with a Shimadzu system equipped with a CMB-20A controller system, an SIL-20A HT autosampler, and LC-20AT tandem pump system, a DGU-20A degasser unit, a CTO-20AC column oven, an RDI-10A refractive index detector, and two Waters Styragel columns (HT3 and HT4). Each column was 300 mm × 7.8 mm^2, providing an effective molar mass range from 500 to 600 k Da. DMAc containing 4.3 g/L lithium bromide was used as the eluent with a flow rate of 1 mL/min at 40 °C. The Number-average molecular weight (Mn) and polydispersity index (Đ) were calculated using Shimadzu LC Solution software. The GPC columns were calibrated with low dispersity poly(methyl methacrylate) (PMMA) standards (Polymer Laboratories)

Cryogenic Transmission Electron Microscopy (Cryo-TEM)
Cryo-EM grids were prepared by applying 4 ul of nanoparticle containing solutions on 1.2/1.3 holey carbon grid (Quantifoil Micro Tools GmbH; Großlöbichau, Germany) which were glow discharged before sample application in a Pelco easiGlow device (Ted Pella; Redding, California) at 30 mA for 30 s. The grids were then blotted using a Vitrobot mark IV (Thermo Fischer Scientific) using a setting of -3 blot force and 3 sec blot time at 100% humidity and 4 °C and plunge frozen in liquid ethane to obtain the vitrified samples. Cryo transmission electron microscopy was performed using a FEI Tecnai Spirit G2 TEM (Thermo Fischer Scientific), operated at 120keV.

Ultraviolet-Visible (UV-Vis) Spectroscopy
UV-Vis spectra from 400 to 800 nm were collected on an Agilent Technologies Cary 60 UV-Vis using standard Macro Fluorescence cuvettes.

Fourier-transform infrared (FT-IR) Spectroscopy
FT-IR spectra were collected on a Perkin Elmer ART-FTIR and signals are listed as wavenumber (cm^{-1}).

Nanoparticle Tracking Analysis (NTA)
Nanoparticle concentrations were analyzed using the NS300 Nanosight (Malvern Instruments) via five measurements. The camera level was set to 8, the screen gain to 7, and the detection threshold to 7.

Cell Viability.
Human embryonic kidney (HEK) cells, human dermal fibroblast (HDF) cells and J774A.1 macrophages were all obtained from American Type Culture Collection (ATCC).

Nanoparticle concentrations for Cell Viability.
Without accounting for material losses during the dialysis purification process, the polymer mass concentration of all nanoparticles used for Cell Viability assays was approximately 500 µg polymer/mL, corresponding to 50 $\times 10^9$ particles/mL in **Figure 6.** In terms of POM mass concentration, the highest concentrations of POM used in this study were *c.a.* 8 µg/mL (1%POM@NPs, 50×10^9 particles/mL), 25 µg/mL (3.5%POM@NPs, 50×10^9 particles/m), and 40 µg/mL (5%POM@NPs, 50×10^9 particles/mL), respectively.

In vitro testing of HEK cells.
HEK cells were seeded at 10,000 cells per well in clear-bottom 96-well black plates and incubated overnight at 37 °C with 5 % CO_2. The cells were then treated with nanoparticles at eight different concentrations 37 °C for 72 h with 5 % CO_2. After incubation, the media was removed and a 10 % v/v solution of AlamarBlue in DMEM was added. The cells were incubated for a further 3 h at 37 °C. Cell viability was determined by measuring the fluorescence at 590 nm using a fluorescence plate reader (Clariostar, BMG). Control samples were cells incubated with DMEM (without nanoparticles). The viability was calculated using the equation below, where FI=fluorescence intensity.

$$\text{Cell viability (\%)} = \frac{(\text{FI sample} - \text{FI blank})}{(\text{FI control} - \text{FI blank})} \times 100$$

(FI sample – FI blank)/(FI control – FI blank) × 100%

In vitro testing of HDF cells and J774A.1 macrophages.
Resazurin was used for the determination of the percentage viability of all cell types. Volumes of 10^5 fibroblasts and/or macrophages/mL were initially plated into 96-well plates and left for 24 hours to adhere. Working stock solutions were generated by solubilising polyoxometalate loaded nanoparticles to 1 x 10^{11} particles/mL in PBS. Stock solutions were then sequentially diluted out in the appropriate culture media in a separate well plate to give a maximum concentration of 5.00 x 10^{10} particles/mL. All compounds were analysed in duplicate per well-plate (eg compound A in rows A and B, B in C and C . . . etc). The old media was discarded form the cell plates and the compound gradient media pipetted into the cell plates. Plates were then incubated at 37°C in 5% CO_2. At the approximate time point (24 or 48 hours) resazurin at the appropriate concentration in sterile PBS was added. Plates were incubated for a further 4 hrs and then spectroscopically measured on a ThermoFisher VarioSkan Lux using fluorescence excitation at 560 nm and emission at 590 nm. This was compared against a positive control of untreated cells to determine the percentage inhibition

using the same equation applied to the HEK cell line.

Synthesis

The polyoxometalate (POM), $(TOA)_{6-x}H_x[B^{III}W_{11}O_{39}Co^{III}]$, and pyridin-4-yl methyl methacrylate (PyMMA) used in this study were prepared as described previously in the literature.[1-2] All other materials were prepared by modification of literature procedures or used as purchased where indicated.

Poly(ethylene glycol methacrylate) (PEGMA) macro RAFT agent)
PEGMA (average Mn 300 Da) (2 g, 6.67 mmol), azobisisobutyronitrile (AIBN) (1.47 mg, 9.5 μmol) and 4-cyano-4-[(dodecylsulfanylthio-carbonyl)sulfanyl]pentanoic acid (38.5 mg, 95.3 μmol) were dissolved in 1,4-dioxane (4 g) and placed into a Schlenk flask equipped with a magnetic stirrer bar. The flask was degassed by four freeze–pump–thaw cycles (5min, 10min, 15min, 20min). The mixture was stirred at 60 °C for 14 h with the reaction terminated by exposure to air. The polymer was purified by precipitation from cold n-hexane, washed with cold n-hexane and subsequently dried under reduced pressure. The molecular weight of PEGMA macro RAFT agent was determined by ^{1}H NMR (400 MHz, $CDCl_3$) to be approximately 12 kDa.
^{1}H NMR (400 MHz, $CDCl_3$) δ 4.08 (-COO-C**H$_2$**-CH_2-), 3.66 (PEG backbone), 3.55 (-COO-CH_2-C**H$_2$**-O-C**H$_2$**-), 3.38 (-O-C**H$_3$**), 1.90-1.75 (backbone-C**H$_2$**-C-CH_3), 1.25 (-CH_2-C_8**H$_{16}$**-CH_2-), 1.05-0.82 (backbone-CH_2-C-C**H$_3$**).

Poly(ethylene glycol methacrylate)-*b*-poly(2-(diethylamino)ethyl methacrylate) (PEGMA-*b*-PDEAEMA) shell polymer (SP): DEAEMA (1 g, 5.4 mmol), AIBN (0.44 mg, 2.7 μmol) and PEGMA macro-RAFT agent (270 mg, 22.5 μmol) were dissolved in 1,4-dioxane (2 g) and placed into a Schlenk flask equipped with a magnetic stirrer bar. The flask was degassed over four freeze–pump–thaw cycles (5min, 10min, 15min, 20min). The mixture was stirred at 60 °C for 24 h with the reaction terminated by exposure to air. The polymer was purified by precipitation from cold n-hexane, washed with cold n-hexane and subsequently dried under reduced pressure. The molecular weight of SP was determined by ^{1}H NMR (400 MHz, $CDCl_3$) to be approximately 25 kDa (**Figure S1**).The dispersity (Đ) of SP was determined by SEC to be approximately 1.23 (**Figure S6**).
^{1}H NMR (400 MHz, $CDCl_3$) δ 4.05 (PEGMA-COO-C**H$_2$**-CH_2-), 3.97 (PDEAEMA-COO-C**H$_2$**-CH_2-), 3.63 (PEG backbone), 3.54 (PEGMA-COO-CH_2-C**H$_2$**-O-C**H$_2$**-), 3.36 (-O-C**H$_3$**), 2.68 (-CH_2-C**H$_2$**-N-), 2.55 (-N-C**H$_2$**-CH_3), 1.90-1.75 (backbone-C**H$_2$**-C-CH_3), 1.23 (-CH_2-C_8**H$_{16}$**-CH_2-), 1.02(-N-CH_2-C**H$_3$**), 1.05-0.80 (backbone -CH_2-C-C**H$_3$**).

In this study, a library of coordination polymers (CPs) was synthesized via RAFT polymerization, which were named based on the ratio of (pyridyl)methyl methacrylate (PyMMA) they contained. For instance, a CP with 5 mol% PyMMA was designated as 5%Py@CP. Here is an example of the synthesis of **5%Py@CP**. **Poly(2-**

(dimethylamino)ethyl methacrylate-*r*-2-(diisopropylamino)ethyl methacrylate)-*r*-pyridin-4-ylmethyl methacrylate) (P(DEAEMA-*r*-DPAEMA-*r*-PyMMA)) (5%Py@CP): DEAEMA (1 g, 5.4 mmol), DPAEMA (1.15g, 5.4mmol), PyMMA(93mg, 0.54mmol), AIBN (0.70 mg, 4.3 μmol) and RAFT agent (112 mg, 43.2 μmol) were dissolved in 1,4-dioxane (4.3 g) and placed into a Schlenk flask equipped with a magnetic stirrer bar. The flask was degassed over four freeze–pump–thaw cycles (5min, 10min, 15min, 20min). The mixture was stirred at 60 °C for 24 h with the reaction terminated by exposure to air. The polymer was purified by precipitation from acetonitrile, washed with cold acetonitrile and subsequently dried under reduced pressure. The molecular weight of 5%Py@CP agent was determined by ^{1}H NMR (400 MHz, $CDCl_3$) to be approximately 29.5 kDa. **(Figure S4)** The dispersity (Đ) of SP was determined by SEC to be approximately 1.25. **(Figure S9)**
^{1}H NMR (400 MHz, $CDCl_3$) δ 8.61(py-**H**) , 7.24(py-**H**), 4.96 (PyMMA-COO-C**H$_2$**-py), 3.99 (PDEAEMA-COO-C**H$_2$**-CH_2-), 3.82 (PDPAEMA-COO- C**H$_2$**-CH_2-), 2.98 (-N-C**H**-$(CH_3)_2$), 2.70 (-CH_2-C**H$_2$**-N-), 2.58 (-N-C**H$_2$**-CH_3), 2.10-1.70 (backbone-C**H$_2$**-C-CH_3), 1.23 (-CH_2-C_8**H$_{16}$**-CH_2-), 0.99 (-N-CH_2-C**H$_3$**), 1.10-0.80 (backbone-CH_2-C-C**H$_3$**).

Formation of coordination bonds
TOA salts of POM (0.22 μmol, 0.54 μmol, and 1.07 μmol) was added to a 0.17 mM acetone stock solution (900 μL) of each CP (4.5 mg, 0.15 μmmol). The POM-CP solution was incubated at 45°C for achieving maximum coordination. Following heating, cooling did not result in any changes to the spectra indicating the thermodynamic stability of the coordinate bonds between POM and polymer bearing pyridyl functionality.

Formation of the control nanoparticles
Shell polymer (1.5 mg) and core polymer (1.5 mg) were dissolved in 300 μL acetone. The mixture was added into 3 ml PBS (0.1M, pH 8) then transferred to a 100 kDa molecular weight cut-off dialysis tube and dialyzed against 1000 ml PBS (0.1M, pH 8) for 24 hours with six changes of dialysis solution. The nanoparticles were removed and stored at r.t. for 24h and filtered through a 0.45 μm PES filter before use.

Formation of the POM-polymer hybrid nanoparticles
Shell polymer (1.5 mg, 0.06 mmol) was added into a stock solution of POM-CP in acetone (300 μL, 0.05 mmol with respect to CP). The mixture was then added dropwise into 3 mL PBS over a period of 30 seconds and stirred for an additional five minutes after complete addition. The same purification procedures were conducted as the control group before any characterization.

Figures

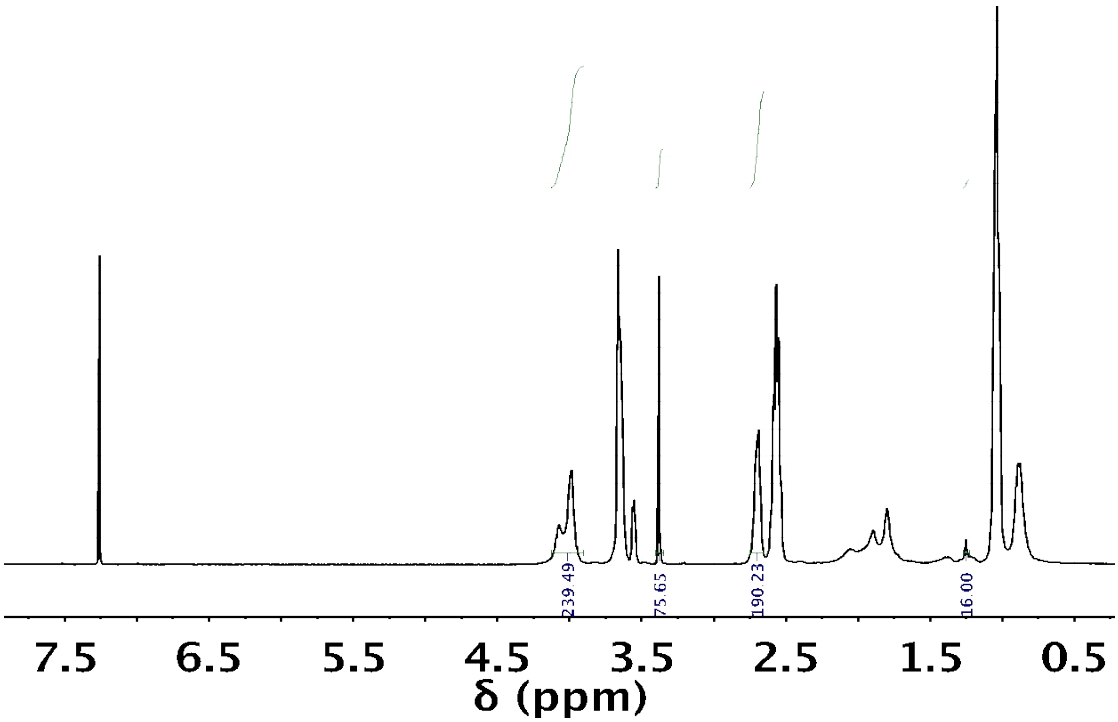

Figure S1. ^{1}H NMR of Poly(ethylene glycol methacrylate)-*b*-poly(2-(diethylamino)ethyl methacrylate) (SP) in $CDCl_3$.

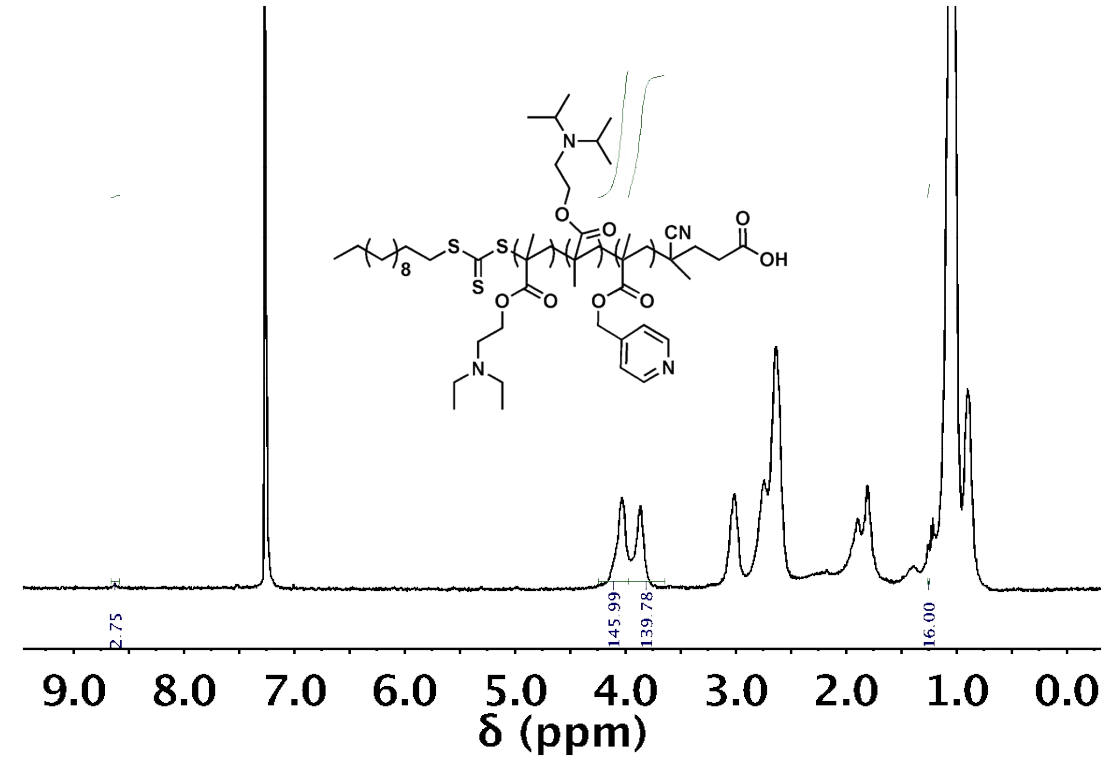

Figure S2. ^{1}H NMR of Poly(2-(diethylamino)ethyl methacrylate-*r*-2-(diisopropylamino)ethyl methacrylate-*r*-pyridin-4-ylmethyl methacrylate) (CP) bearing 1% pyridyl functionality in $CDCl_3$.

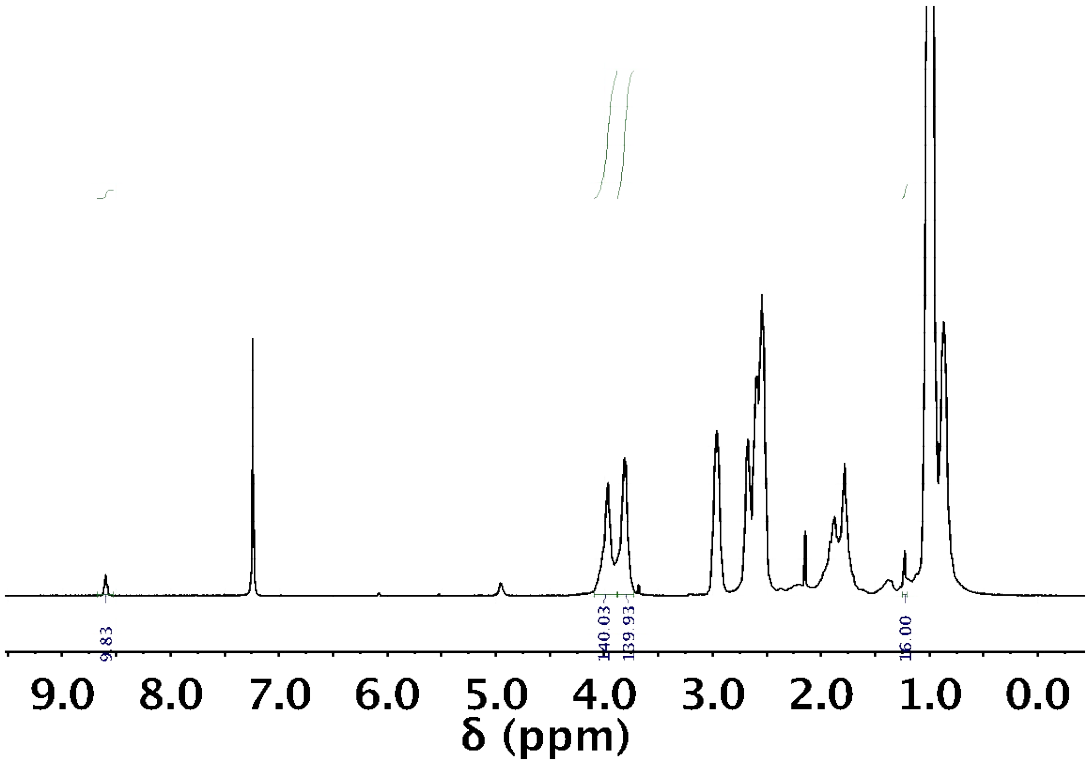

Figure S3. ^{1}H NMR of Poly(2-(diethylamino)ethyl methacrylate-*r*-2-(diisopropylamino)ethyl methacrylate-*r*-pyridin-4-ylmethyl methacrylate) (CP) bearing 3.5% pyridyl functionality in $CDCl_3$.

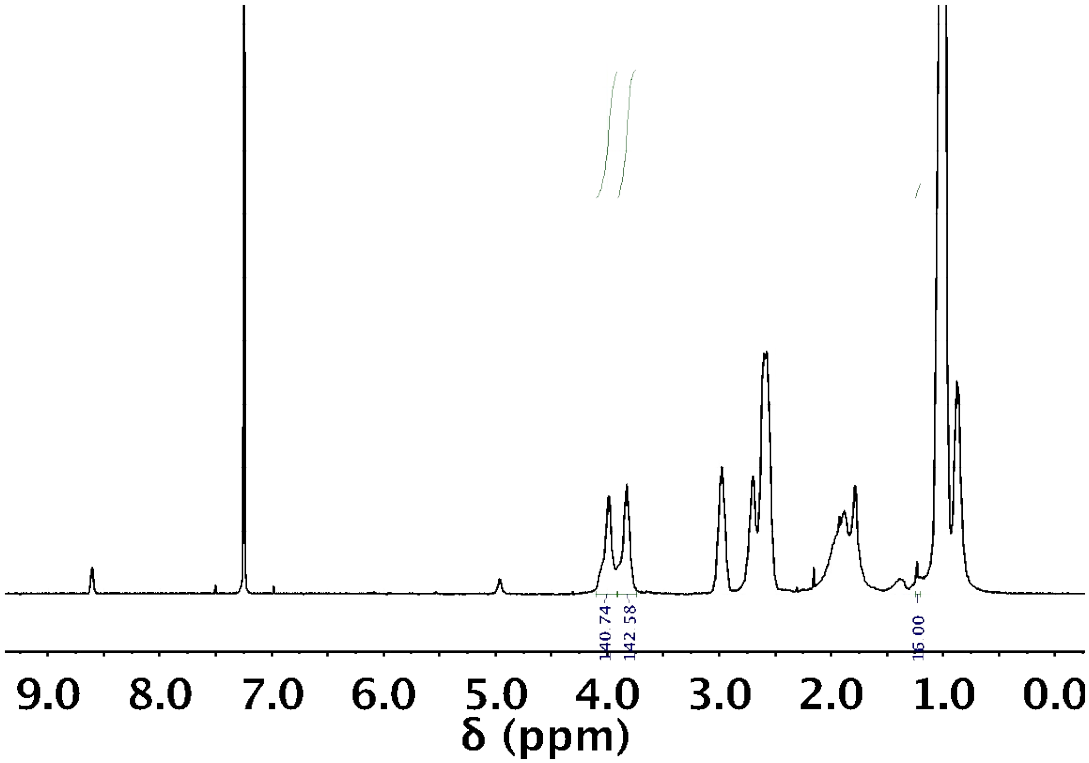

Figure S4. ^{1}H NMR of Poly(2-(diethylamino)ethyl methacrylate-*r*-2-(diisopropylamino)ethyl methacrylate-*r*-pyridin-4-ylmethyl methacrylate) (CP) bearing 5% pyridyl functionality in $CDCl_3$.

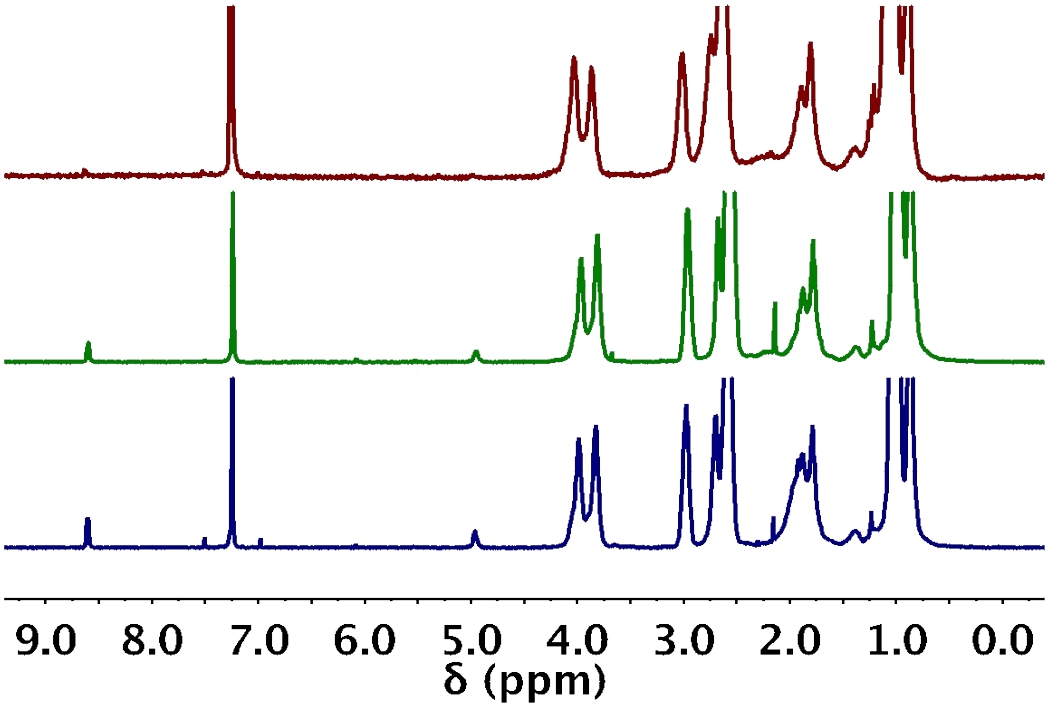

Figure S5. Stacking ^{1}H NMR spectra of 1%Py@CP (red), 3.5%Py@CP (green), and 5%Py@CPs (blue) in $CDCl_3$. The increasing resonance of pyridyl alpha-proton of CP (see peak d in Figure S2) was highlighted using a dashed box.

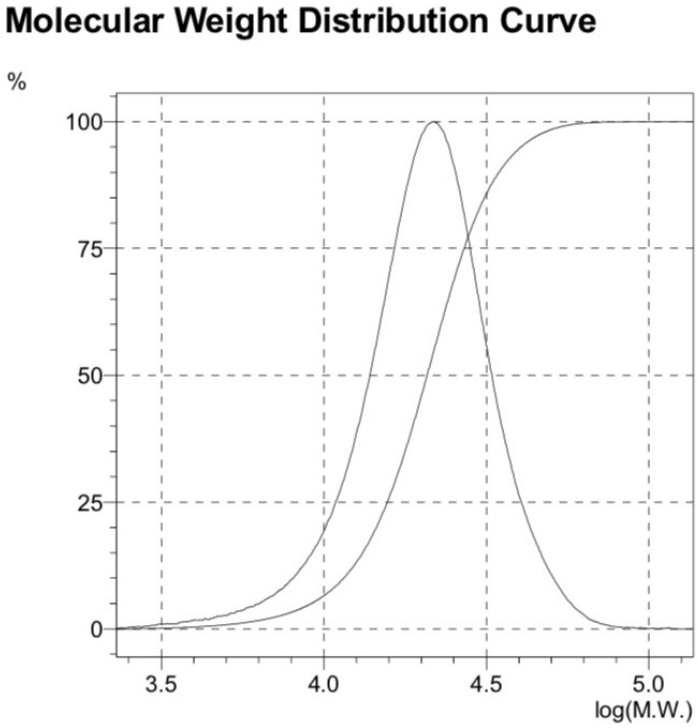

Figure S6. SEC trace and calibration curve of shell polymer.

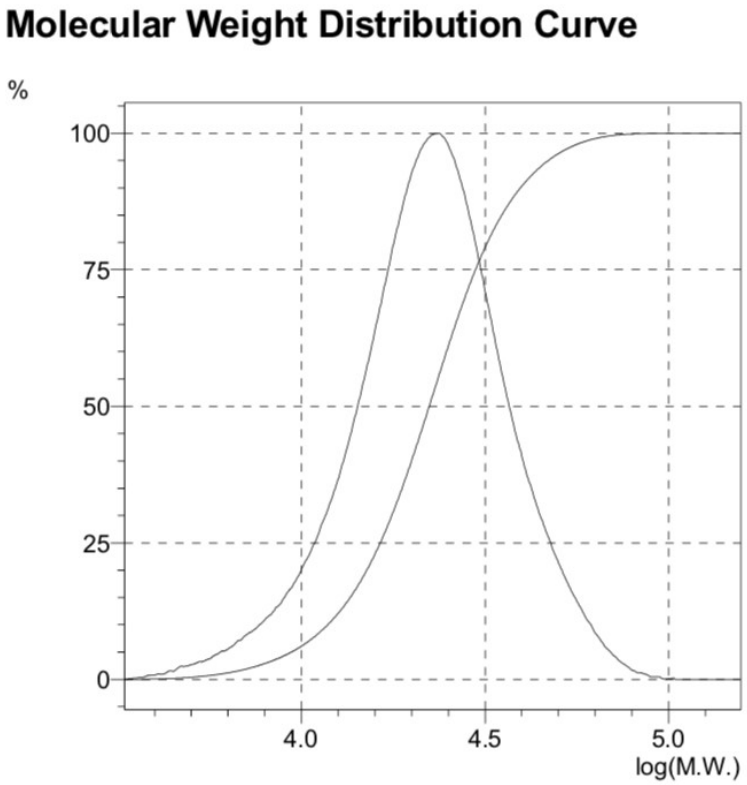

Figure S7. SEC trace and calibration curve of 1% Py@CP

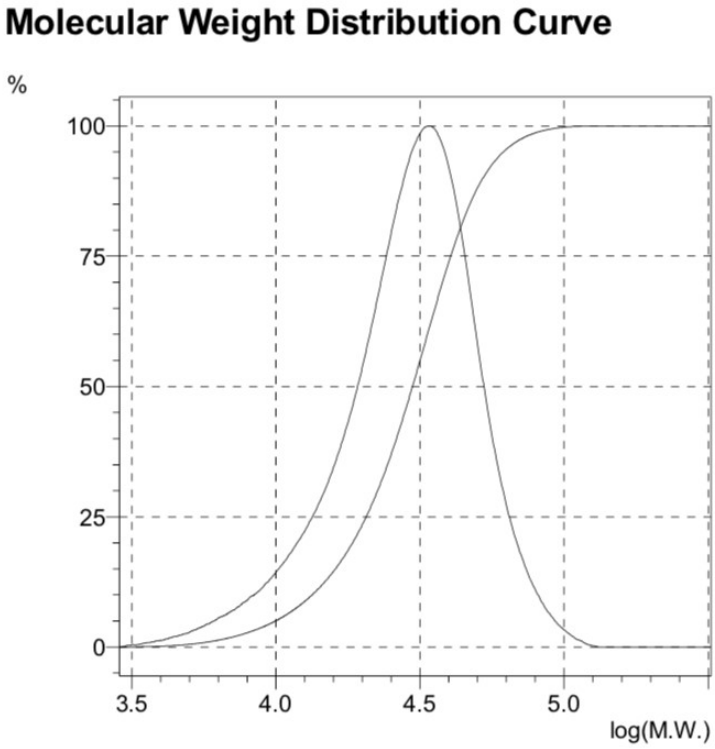

Figure S8. SEC trace and calibration curve of 3.5% Py@CP.

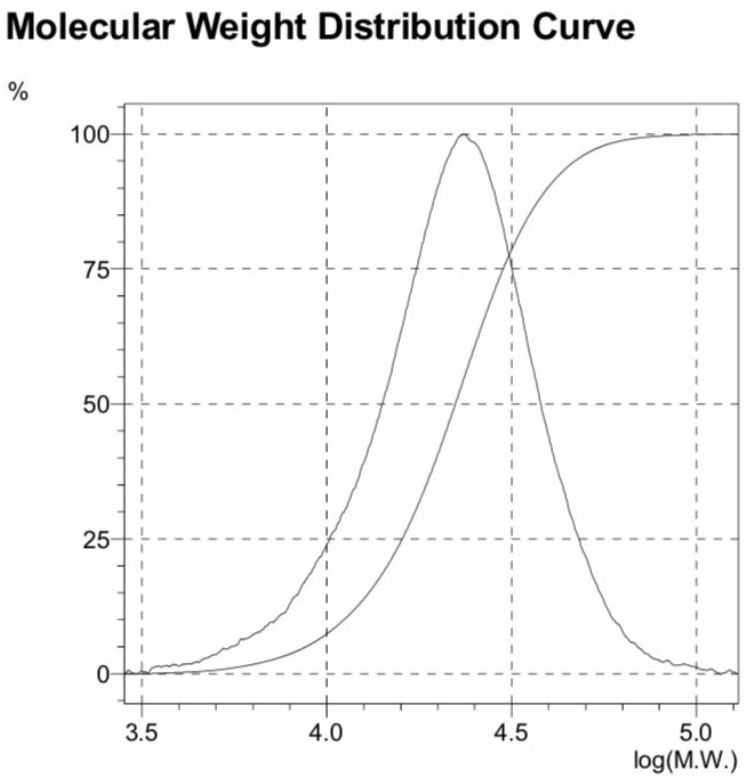

Figure 9. SEC trace and calibration curve of 5% Py@CP.

Table S1. Characterization of polymers synthesized in this study

Polymer	M_n (kDa, NMR)	M_n (kDa, SEC)	M_w (kDa, SEC)	*Đ*
SP	25.7	18.1	22.2	1.23
1% Py@CP	28.7	19.4	24.3	1.25
3.5% Py@CP	29.2	24.6	31.9	1.30
5% Py@CP	29.5	24.4	30.6	1.25

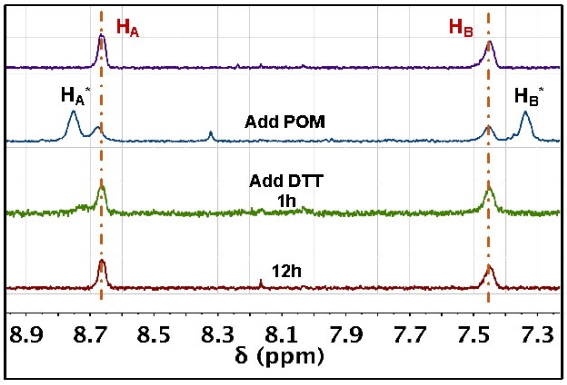

Figure S10. ^{1}H NMR of 1%Py@CP in Acetone-d_6, showing the change in the chemical shift of the pyridyl alpha- (H_A) and beta-protons (H_B) on coordination of POMs. *denotes coordination.

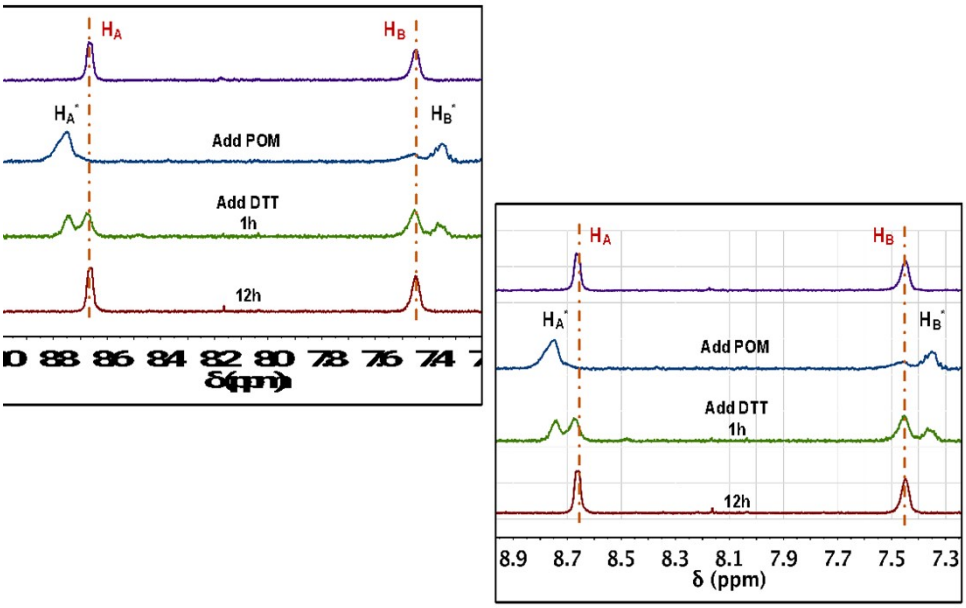

Figure S11. ^{1}H NMR of 3.5%Py@CP in Acetone-d_6, showing the change in the chemical shift of the pyridyl alpha- (H_A) and beta-protons (H_B) on coordination of POMs. *denotes coordination.

Figure S12. Visual image of POM-CP stock solutions (right) and the color change after the addition of DTT (left).

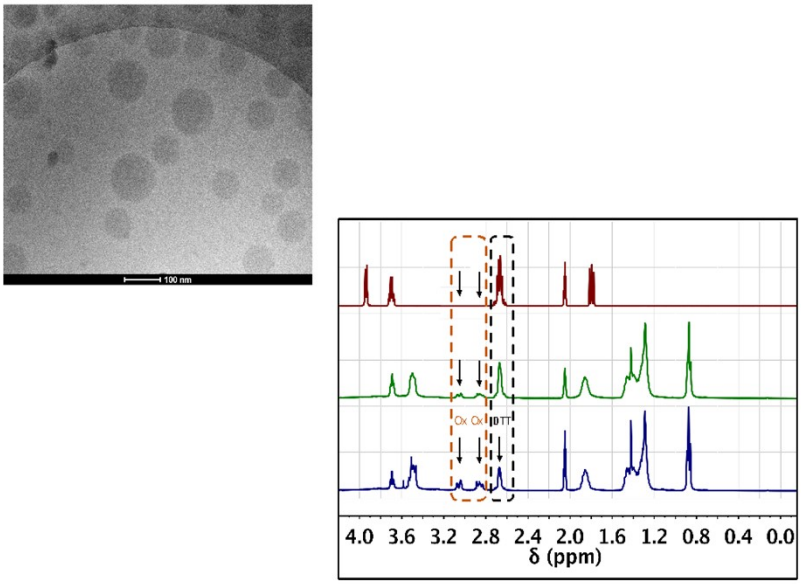

Figure S13. ^{1}H NMR of DTT in Acetone-d_6 (red line), and after addition of TOA salts of POM for 1h (green) and 12 h (blue). The peaks belonging oxidized DTT were identified and labeled in the figure.

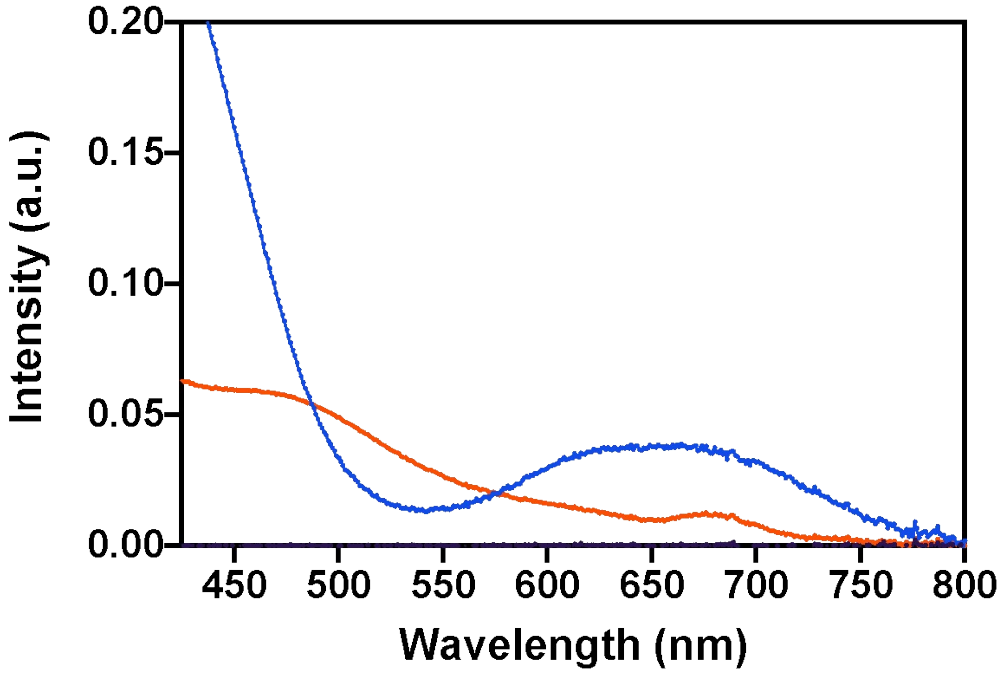

Figure S14. UV-Vis spectra of $Ba_3[B^{III}W_{11}O_{39}Co^{III}(H_2O)]$ (blue, λ_{max} - 660 nm), and the reduction product after the addition of DTT (orange, λ_{max} - 480 nm) in water.

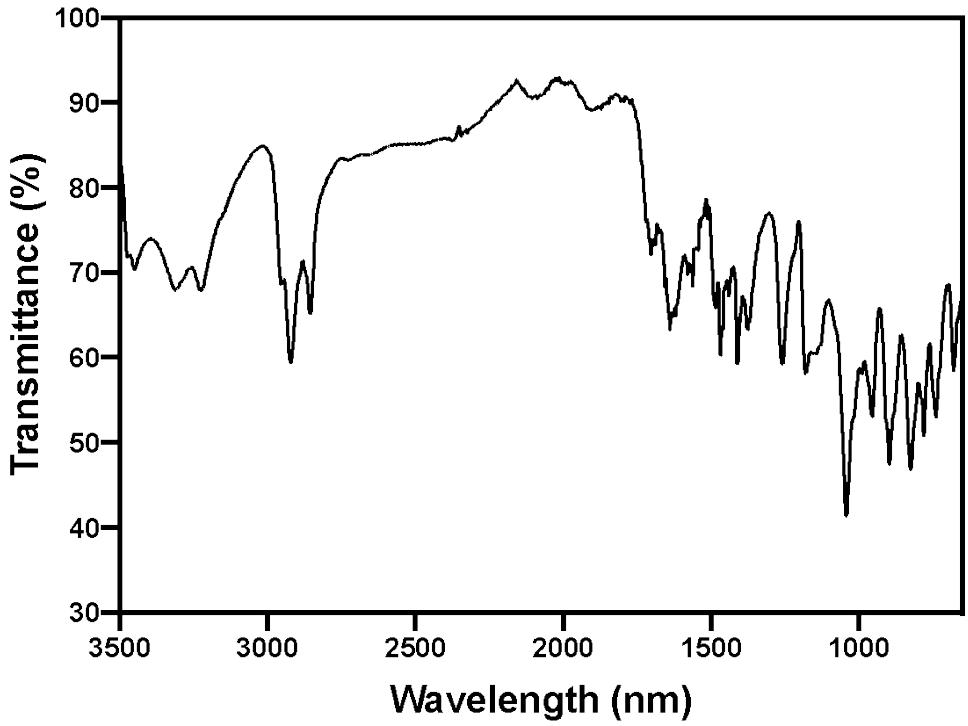

Figure S15. FT-IR spectrum of the reduction product of $[B^{III}W_{11}O_{39}Co^{III}(H_2O)]^{6-}$ after the addition of DTT.

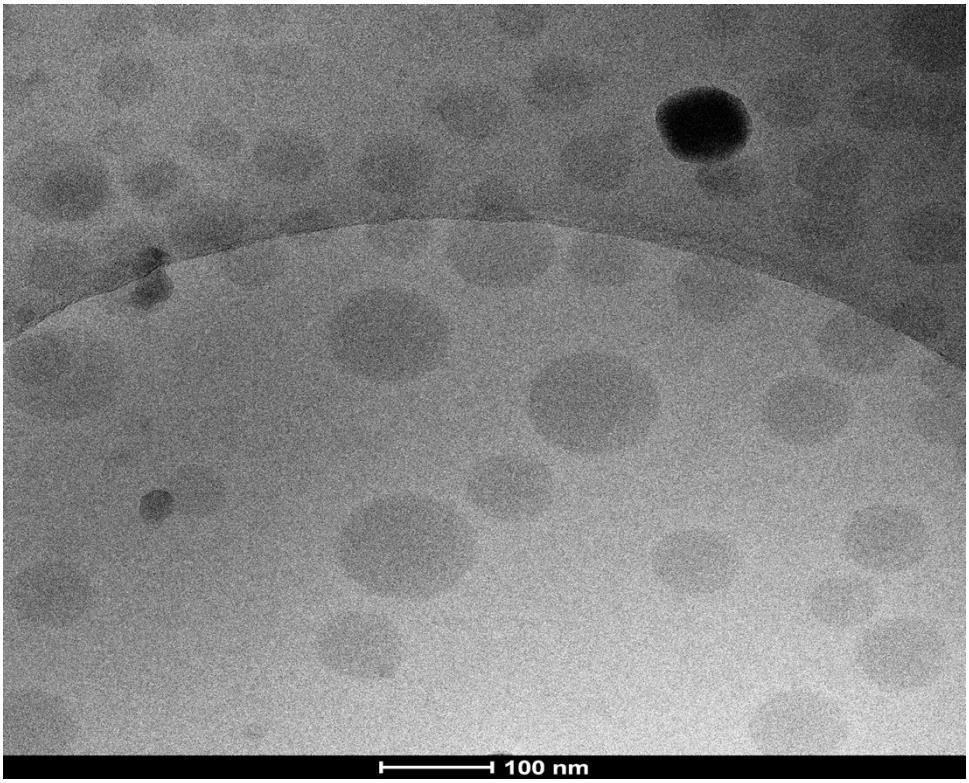

Figure S16. Representative Cryo-EM image of control (no POM modified) nanoparticles.

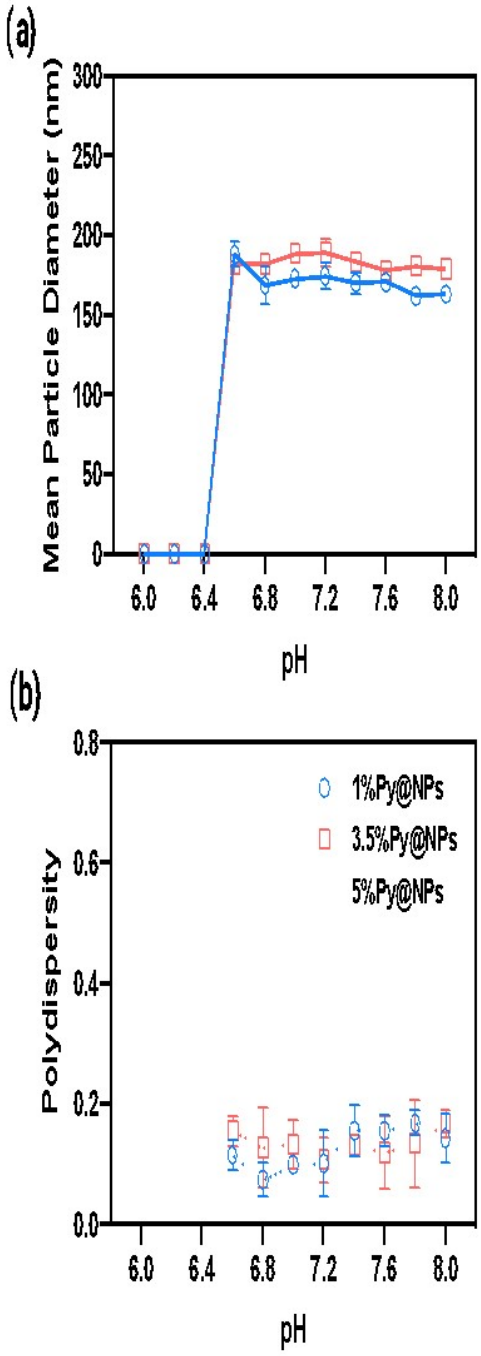

Figure S17. pH disassembly profiles of control nanoparticles, 1%Py@NPs (light blue), 3.5%Py@NPs (light red) and 5%Py@NPs (light green), in the pH range 8.0-6.0. (a) Mean particles diameter; (b) Polydispersity of nanoparticles. Error bars represent the standard deviation of the mean, calculated from three independent replicates (n=3)

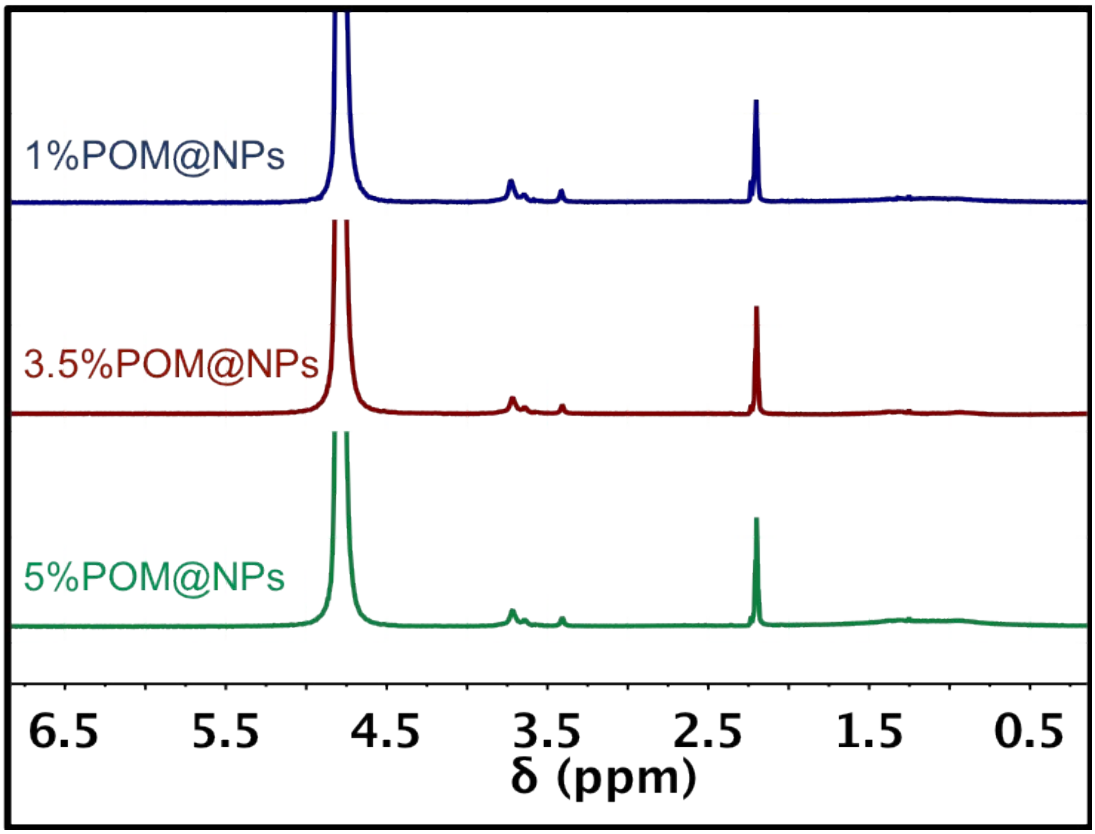

Figure S18. ^{1}H NMR of 1%POM@NPs (blue), 3.5%POM@NPs (red), and 5%POM@NPs (green) in pH 7.4 PBS prepared using D_2O. Resonances for the core polymer are not observed due to the significantly shorter T2.

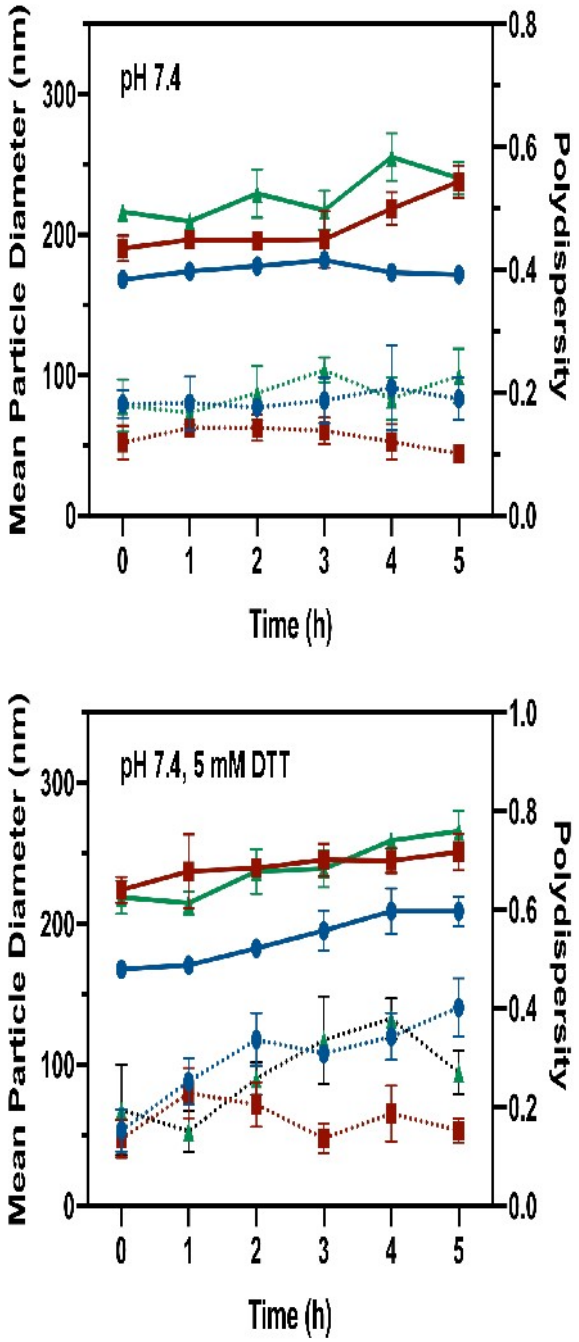

Figure S19. Stability tests of 1%POM@NPs (blue), 3.5%POM@NPs (red) and 1%POM@NPs for 5h measured by DLS at pH 7.4 in the presence (bottom) or absence of DTT (top). Solid lines represent mean particle diameter and dotted lines represent polydispersity. Error bars represent the standard deviation of the mean, calculated from three independent replicates (n=3)

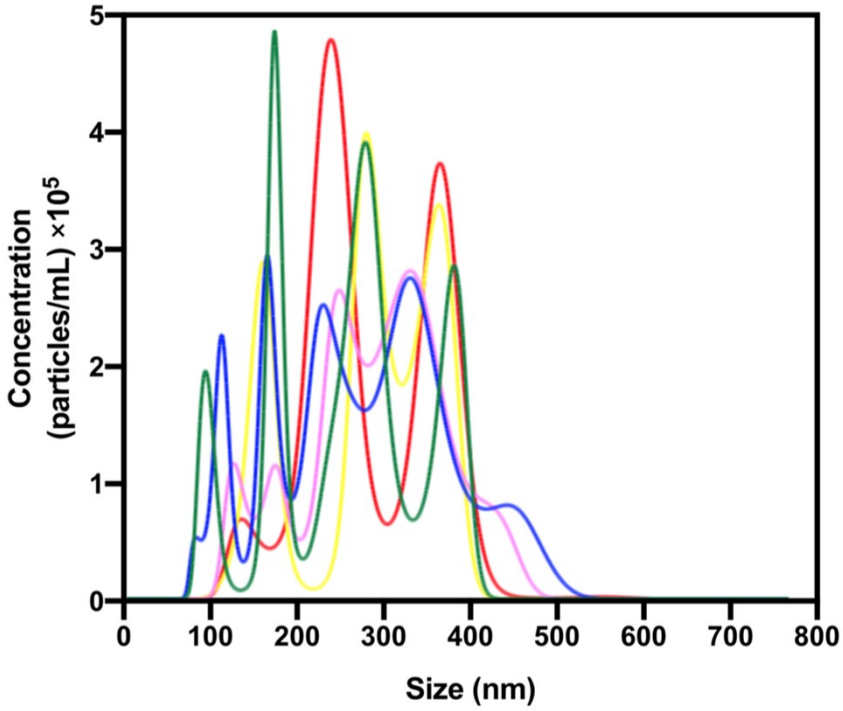

Figure S20. The concentration and size distribution of 1%POM@NPs at pH 6.0 measured by NTA.

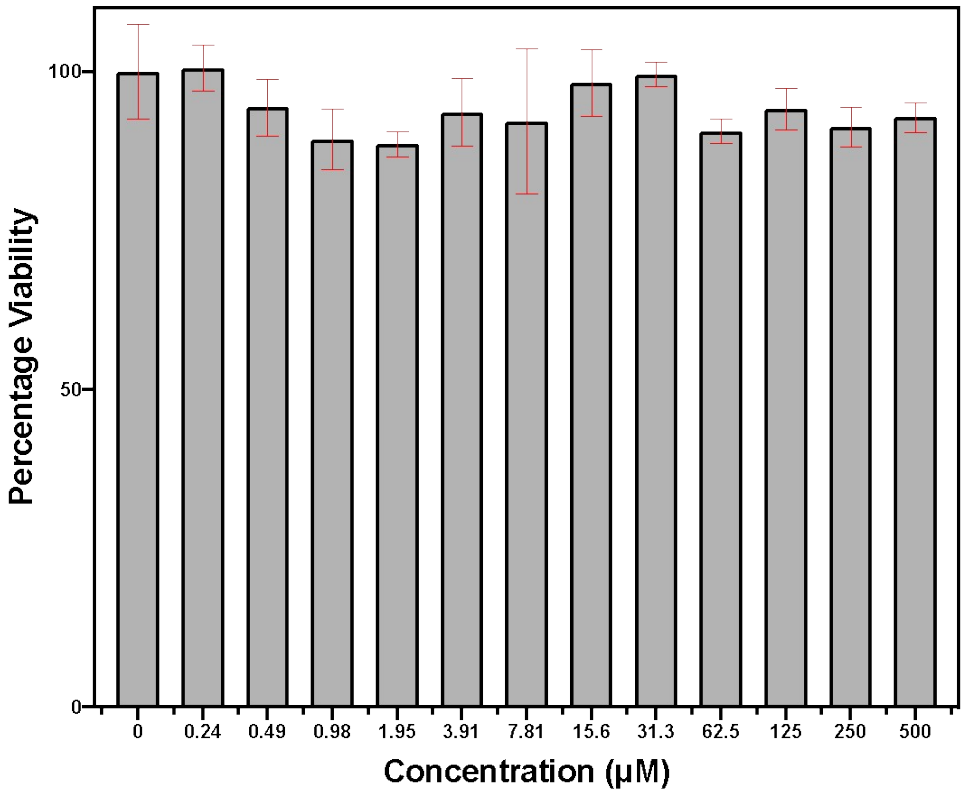

Figure S21. *In vitro* cellular cytotoxicity of $Ba_3[B^{III}W_{11}O_{39}Co^{III}(H_2O)]$ with HEK cells. Error bars represent the standard deviation of the mean, calculated from three independent replicates (n=3)

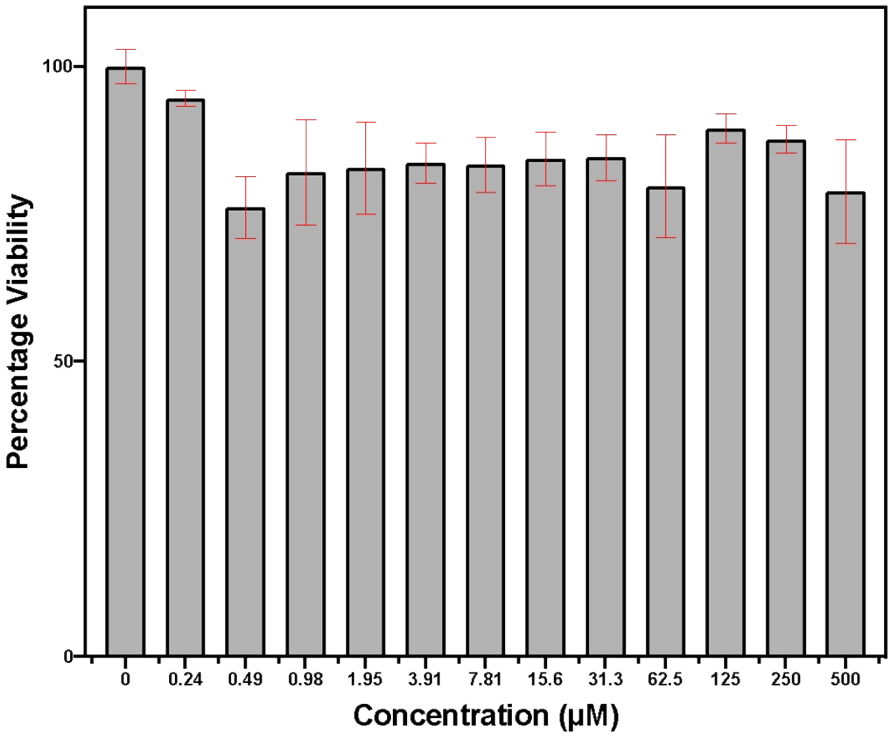

Figure S22. *In vitro* cellular cytotoxicity of $Ba_3[B^{III}W_{11}O_{39}Co^{III}(H_2O)]$ with HDF cells. Error bars represent the standard deviation of the mean, calculated from three independent replicates (n=3)

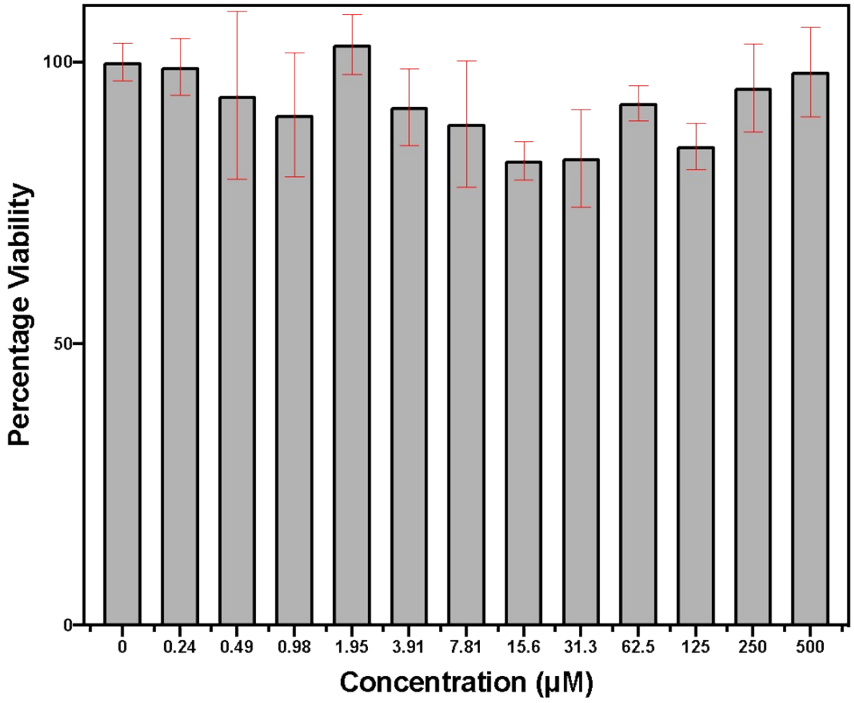

Figure S23. *In vitro* cellular cytotoxicity of $Ba_3[B^{III}W_{11}O_{39}Co^{III}(H_2O)]$ with J774.1A macrophages. Error bars represent the standard deviation of the mean, calculated from three independent replicates (n=3)

Reference

(1) Gao, Y.; Xu, J.; Zhang, C.; Venugopal, H.; Kermaniyan, S. S.; Such, G.; Ritchie,

C. Rationale Design of pH-Responsive Core–Shell Nanoparticles: Polyoxometalate-Mediated Structural Reorganization. *ACS Applied Nano Materials* **2020,** *3* (11), 11247-11253.
(2) Xu, J.; Volfova, H.; Mulder, R. J.; Goerigk, L.; Bryant, G.; Riedle, E.; Ritchie, C. Visible-light-driven “on”/“off” photochromism of a polyoxometalate diarylethene coordination complex. *Journal of the American Chemical Society* **2018,** *140* (33), 10482-10487.